CONF-840411--5

CONF-840411--5

DE84 004010

ARGONNE NATIONAL LABORATORY
9700 South Cass Avenue
Argonne, Illinois 60439

COMPUTER ANALYSIS OF SODIUM COLD TRAP DESIGN AND PERFORMANCE

by

C. C. McPheeters and D. J. Raue

Chemical Technology Division

November 1983

DISCLAIMER

C. C. MCPHEETERS, MS and D. J. RAUE, Argonne National Laboratory, Argonne, IL 60439, U.S.A.

Computer analysis of sodium cold trap design and performance

Normal steam-side corrosion of steam-generator tubes in Liquid Metal Fast Breeder Reactors (LMFBRs) results in liberation of hydrogen, and most of this hydrogen diffuses through the tubes into the heat-transfer sodium and must be removed by the purification system. Cold traps are normally used to purify sodium, and they operate by cooling the sodium to temperatures near the melting point, where soluble impurities including hydrogen and oxygen precipitate as NaH and Na_2O, respectively. A computer model was developed to simulate the processes that occur in sodium cold traps. The Model for Analyzing Sodium Cold Traps (MASCOT) simulates any desired configuration of mesh arrangements and dimensions and calculates pressure drops and flow distributions, temperature profiles, impurity concentration profiles, and impurity mass distributions. The accuracy of the model was checked by comparing calculated mass distributions with experimentally determined mass distributions from literature publications and with results from our own cold trap experiments. The comparisons were good to excellent in all cases.

INTRODUCTION

1. Recirculating sodium systems, whether small experimental systems or large heat-transfer systems, must have an impurity removal system in operation to prevent buildup of impurity concentrations. The impurities of most concern are hydrogen and oxygen, which originate primarily from steam-generator corrosion, moisture from system-component surfaces, and leakage of air into the system. High concentrations of these impurities in sodium can result in rapid corrosion of the system components or plugging of the flow passages or both. In addition to the corrosion and plugging problems, the background hydrogen concentration must be kept low to allow sensitive detection of steam leaks into the sodium. Hydrogen meters are used for this purpose (ref.1).

2. Normal operation of 2-1/4Cr-1Mo steel as steam generator tubes results in slow, predictable corrosion of the steel by formation of an oxide layer. As the steel oxidizes, hydrogen is liberated from the reaction with water. This hydrogen preferentially enters the steel phase rather than the oxide or water phases. Once in the steel, the concentration gradient causes the hydrogen to diffuse toward and into the sodium. Observations of the hydrogen source in sodium systems operated with steam generators have shown that essentially all of the hydrogen produced by this corrosion mechanism enters the sodium rather than the steam (ref.1,2). This hydrogen source requires some improvement in the conventional cold-trap design and operation, such as a significant increase in size, frequent cold-trap changes, in situ regeneration to remove the hydrogen, or an increase in the capacity of the cold trap by design improvements. The objective of this study was to develop a computer model that would facilitate the latter option.

COMPUTER MODEL DESCRIPTION

3. One of the first decisions in developing the Model for Analyzing Sodium Cold Traps (MASCOT) was to use the general configuration of the traditional design including: (1) sodium inlet at the top, (2) downflow in an annulus with cooling on the outer surface of the annulus, (3) counter-current flow of the coolant upward on the outer surface of the cold trap, (4) a bottom region where the downward flow from the annulus turns around and flows upward into the center region, (5) a center, cylindrical section with upward sodium flow and sodium exit at the top, and (6) a flow divider between the center section and the annulus. Within this general structure, it is possible to simulate a large variety of dimensions and packing density arrangements. For convenience, NaK alloy was selected as the coolant, and it is considered to flow in a coolant jacket surrounding the cold trap.

4. The divider wall can be made either conducting or insulating, depending on the case being run. The wire mesh packing can be specified in terms of wire diameter, packing density, and location. Three separate wire diameters and packing densities may be used in each simulation, and the position of each of these packing densities may be specified. The special case of no packing may be specified

for either the annulus or the center section or both. A special case consisting of once-through flow (with no return flow up the center section) can be simulated by making the center section very small and the annulus section very large. The mass deposited in the center section can then be ignored, and the annulus section represents the once-through cold trap. Other special cold-trap configurations, such as radial flow with (1) sodium inlets on the O.D. or (2) holes in the divider wall to short-circuit some of the sodium flow, cannot be simulated with MASCOT.

Configuration of cold trap simulation

5. The MASCOT is a two-dimensional simulation of the cold trap configuration. Cylindrical symmetry of the cold trap is assumed, to allow a two-dimensional array to represent the three-dimensional cold trap. The MASCOT uses a 5° slice of the cold trap as shown in Fig. 1. The inlet pressure of the sodium is assumed to be uniform along the radial dimension of the annulus so that the sodium flow is uniformly distributed in the annulus at the beginning of the simulation. The 5° slice is divided into four regions: (1) the center section, (2) the annulus section, (3) the coolant channel, and (4) the bottom section. The entire slice is divided into an array which is 15 columns wide by 40 rows high. The coolant channel is a one-dimensional column which comprises column 15 of the array. The remaining 14 columns are divided, as desired by the

6. Where possible, matrix calculations are done over the entire 14 by 40 array; however, in most cases, such as pressure/flow calculations, each section is calculated separately, and the pressure drop through each section is adjusted until the desired flow is achieved. In the case of temperature calculations, heat is conducted across the divider wall and the outer wall (unless the wall is insulating); however, flow and mass transfer are, of course, prohibited across these boundaries.

General arrangement of logic

7. The computer code is arranged with data input, and preliminary geometric calculations at the beginning. The first major portion of the iteration section is the pressure/flow calculations. A uniform initial flow distribution is assumed, and the resulting pressure profile is calculated. The flow resulting from this pressure profile is then calculated, and this process is repeated until the pressures and flows in each node are unchanging.

8. Once the flows are established, the next step is calculation of the temperatures. The same general approach is used in this calculation as in the pressure calculation. An initial temperature is set throughout the mesh region, and a heat balance is imposed. The temperatures are allowed to relax to their equilibrium values by repeated calculations through the nodes until each node temperature is unchanging.

user, between the center section and the annulus. The bottom section is a one-dimensional row with elements directly corresponding to the 14 columns of the packed section above.

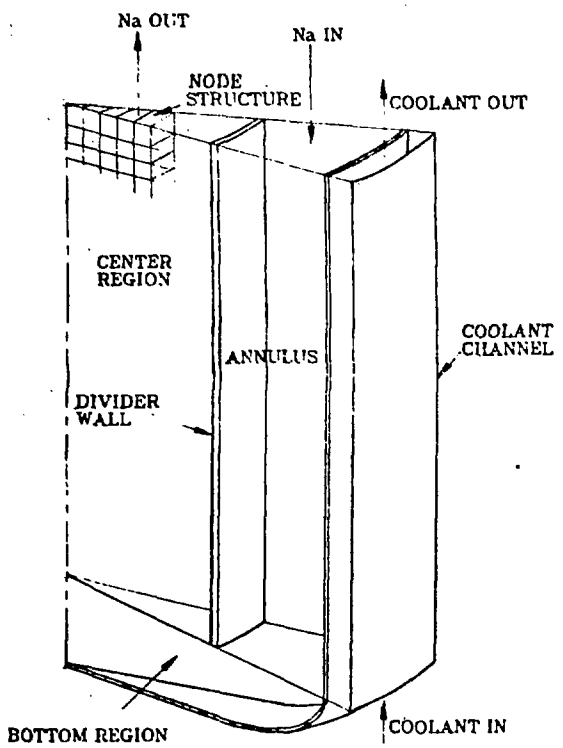

Fig. 1. Five-degree slice of cold trap for model simulation

9. The next step is the impurity concentration distribution. The same general method is used as before. Initial concentration values are set, and these values are allowed to relax to equilibrium values with appropriate mass balance. The situation is more complex in this case, however, because there are two ways mass can leave each node: it can be carried out of the node with the flowing sodium, and it can precipitate on solid surfaces within the node. The concentration calculation continues in an iterative fashion until each node concentration is unchanging.

10. The final step is calculation of the impurity mass deposited in each node. The rate of mass deposition is given by

$$\frac{dm}{dt} = kS(C-C_e) \qquad (1)$$

where m = the impurity mass, t = time, k = the mass transfer coefficient, S = the solid surface area, C = the impurity concentration in solution, and C_e = the equilibrium concentration at the node temperature. In the finite-difference calculation of this model, dt is a fairly large increment of time, and the incremental mass deposited, dm, is also fairly large. The assumption is that the other variables in the equation remain reasonably constant during the time step.

11. At the end of each time step, the computer code returns to the pressure/flow calculation. This process is repeated until either the maximum time specified by the user is reached or the pressure drop through the cold trap exceeds the limit set by the user.

COLD TRAP CASES FROM THE LITERATURE

12. Sodium cold traps have been in use since the 1950s in a wide variety of applications. During that time, several investigators have done thorough analyses to determine the distribution of impurities in [illegible] cold traps after they had become plugged. The primary function of earlier cold traps was perceived to be removal of oxygen from sodium, so the studies were oriented toward the behavior of oxygen. The most important of these studies for our purposes were those of Billuris (ref. 4) and Rogers et al. (ref. 5) and the post-test examination of the Fermi cold trap (ref. 6). In each of these studies, sufficient cold-trap design information is reported to allow simulation with MASCOT, and post-test analyses were done to determine the distribution of the impurities in the plugged cold trap.

Sodium entered the top of the cold trap flowed downward through the packing as oil flowed upward through the coolant channel to remove heat, and the cool, purified sodium exited the cold trap at the bottom. The top of the cold trap was removable so that the interna packing could be removed for analysis after each test. Several types of packing were tested including Raschig rings, wire screen, and (of most interest to us) wire mesh; no packing was also tested. The cold trap was loaded with Na_2O by flowing sodium containing a high concentration of oxygen through the cold trap. This flow was continued until the cold trap became filled and the pressure drop increased to a high enough level to stop the sodium flow.

14. The Billuris experiments were simulated with MASCOT by reading in the cold trap design parameters and the presumed operating conditions. (Unfortunately, the oxygen concentrations were not available.) The MASCOT was run for these conditions until the pressure-drop limit was exceeded. The results were then plotted as shown in Fig. 3. The orientation of Fig. 3 is such that the two-dimensional matrix is on the base

Billuris cold trap tests

13. In the late 1950s, Billuris (ref. 4) conducted a series of basic cold-trap experiments to determine which packing materials would be best for cold trap use. The cold trap that Billuris used in these tests was a simple once-through design with no heat regeneration, as shown in Fig. 2.

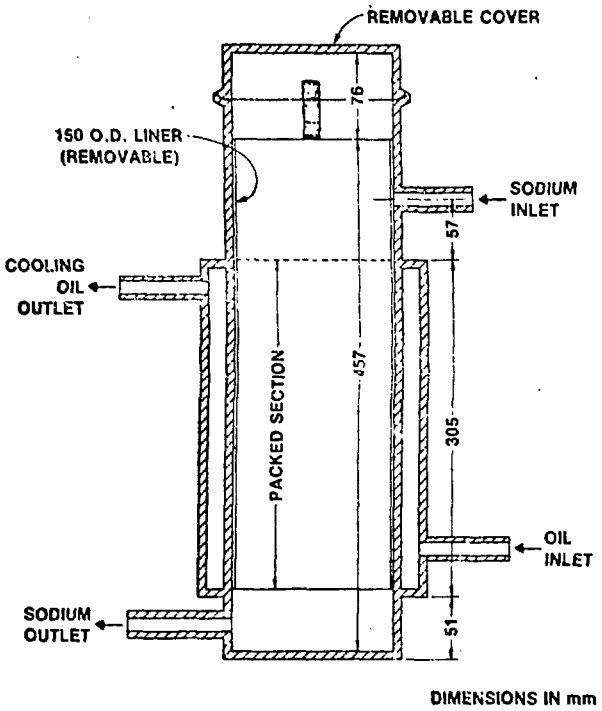

Fig. 2. Billuris cold trap for testing packing materials. Copied with permission from General Electric Company from ref. 4.

plane with the centerline of the cold trap along the back, left edge. The volume percent of Na_2O in each node is plotted vertically at the intersections of the matrix lines. The arrow indicates the sodium flow direction. The experimental results obtained by Billuris are plotted on the back plane of Fig. 3, along with the radial average of the calculated vol % utilizations. While the average curve does not pass directly through the experimental points, it is clear that the general pattern of impurity deposition is in good agreement between the experimental and calculated cases.

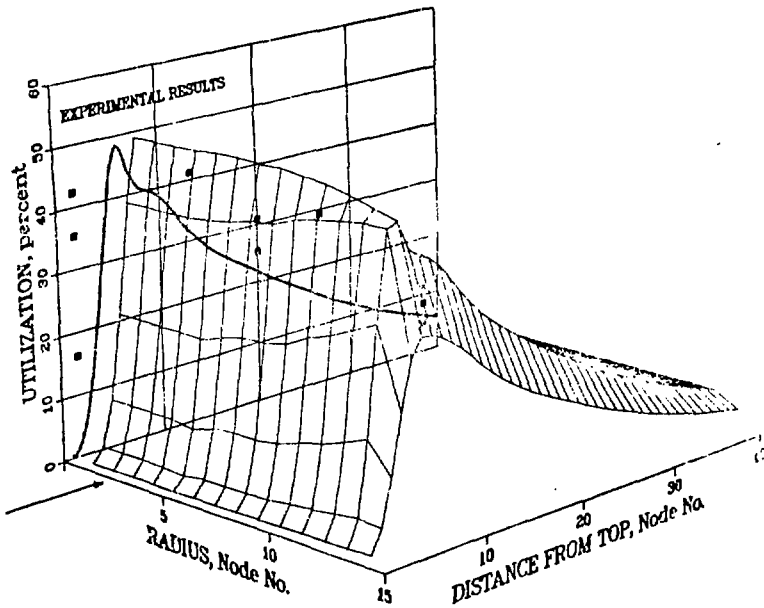

Fig. 3. Impurity mass distribution calculated for the billuris cold trap compared with experimental results.

MSA sodium cold trap tests

15. During the 1960s, Mine Safety Appliances Research Corp. (MSA) conducted a series of tests to determine cold trap behavior in trapping oxygen and carbon. This work was done by Rogers et al. (ref. 5) using an experimental sodium system with cold traps as shown in Fig. 4. The cold trap was of a very simple design that had sodium flow downward through an unpacked, narrow annulus, flow reversal at the bottom, and upward flow through a relatively large packed section in the center. The cold traps used in these experiments were not intentionally loaded with Na_2O, but became loaded in the course of other system operations. After the trap was removed from the system, samples were taken for analysis of the Na_2O distribution. These samples were taken by first drilling through the outer wall and divider wall of the trap, then driving sharpened tubes into the center packed region. The samples were withdrawn and analyzed for Na_2O content.

16. The MASCOT was run using the design

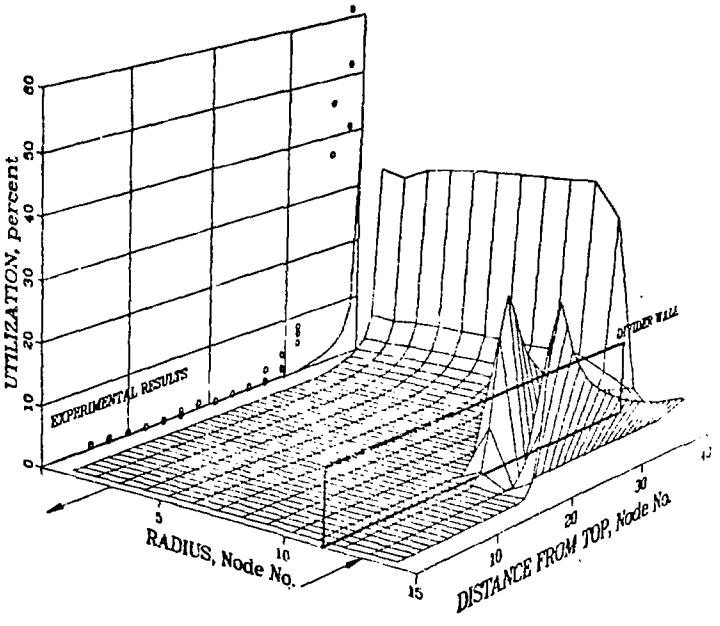

Fig. 5. Impurity mass distribution calculated for the MSA cold trap compared with the experimental results.

parameters and operating conditions of the MSA experiments, and the results of this run are shown in Fig. 5. It was not possible to run this case to plugging (large increase in pressure drop) because of the unusual behavior of Na_2O deposits in the annulus; therefore,

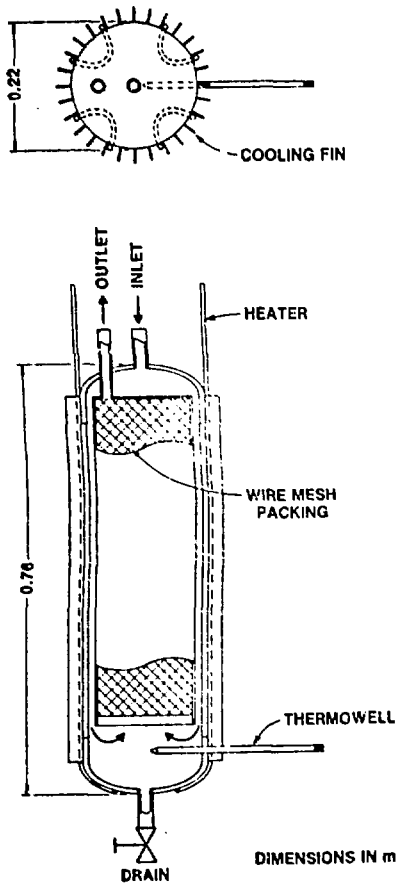

Fig. 4. Cold trap used in the MSA experiments. Copied with permission from MSA Corporation from ref. 5.

the volume utilization reached a maximum of only ~35% at the bottom of the packed section. As in the Billuris case, the calculated Na_2O distribution curve does not pass directly through the experimental points; however, the agreement between the experimental and calculated distributions is good. The Na_2O deposit is concentrated at the bottom of the mesh section in both cases. The reason for this concentration at the bottom of the mesh seems to be that the sodium is cooled below the saturation temperature in the annulus, where little solid surface area is available for precipitation. The solution becomes supersaturated, and, when it enters the mesh, a large surface area is suddenly available and profuse precipitation occurs quickly.

17. An interesting feature of Fig. 5 is the large peaks of mass deposition in the annulus region. The annulus is not packed in this case; thus, the only surface available for precipitation is the wall surface. In the actual cold trap, the Na_2O that deposited on the walls of the annulus probably accumulated to a critical size, then broke off the wall and fell to the bottom of the cold trap. Unsupported Na_2O crystals probably would not have sufficient strength to withstand the hydraulic forces of the sodium flow. This buildup and breakaway phenomenon cannot be modeled with MASCOT.

Fermi reactor cold trap analysis

18. The most extensively analyzed cold trap in this study was the one removed from the primary sodium coolant system of the Fermi reactor (ref. 6) in February 1963. The Fermi cold trap was operated intermittently during the period from January 1960 until its removal. The design configuration, shown

in Fig. 6, was similar to that of the MSA experimental cold trap. Sodium flowed downward through a very narrow annulus that contained no packing material. A counterflow of NaK in the outer jacket cooled the incoming sodium. The sodium flow direction reversed at the bottom of the trap and continued upward through a very large center section packed with wire mesh.

19. After the cold trap on the Fermi system had become plugged, it was removed, and samples were taken for analysis of impurity distributions. These samples were taken by first removing the coolant jacket, then drilling holes through the cold trap outer wall and the divider wall. Sharpened tubes were driven deeply into the center section to sample the sodium and impurity deposits. These tubes were long enough to allow several samples from the same axial position to be analyzed. Unfortunately, the annulus section was not sampled, since the experimenters did not expect to find any impurity deposits in that region. The samples were analyzed for Na_2O content as well as for a variety of

mesh-section calculation could be completed. In the actual cold trap, these deposits would likely have broken off the annulus walls and dropped to the bottom; however, the MASCOT has no mechanism for handling this sequence of events.

21. The Na_2O deposit distribution calculated for the Fermi case is shown in Fig. 7. The first feature that receives our attention, in Fig. 7, is the large deposits in the annulus region. As discussed above, these deposits would probably have spalled off the walls of the actual cold trap, so their significance should be minimized in this calculation. For our purposes, the most important feature of Fig. 7 is the Na_2O distribution in the mesh section. Note that the mass deposition is concentrated in the lower part of the central mesh section and that this location matches, very well, the location in which the Na_2O was found in the actual cold trap. The shaded region represents the range of results from analyses of several samples from each axial location.

other impurities.

20. The design features and operating conditions of the Fermi cold trap were read into the MASCOT, and the case was run. It was not possible to run the case all the way to plugging because of the large buildup of Na_2O deposits in the thin annulus. These large deposits caused calculational instabilities in the program before the

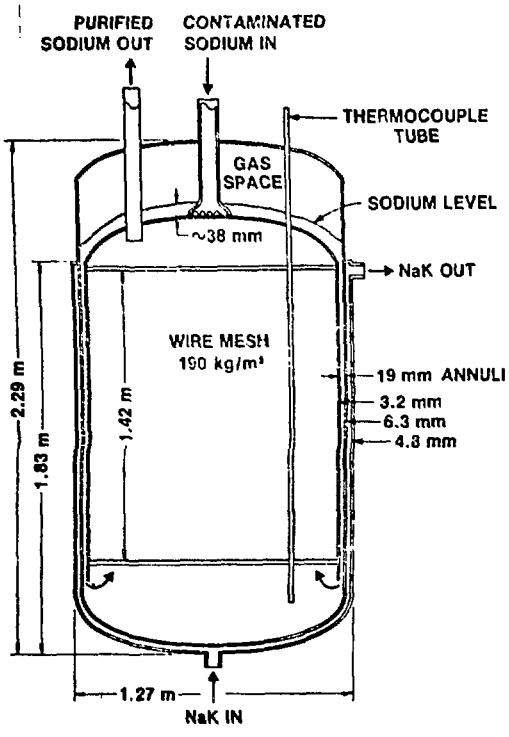

Fig. 6. Design of the Fermi primary system cold trap. Copied with permission from Westinghouse Electric Corporation from ref. 6.

COLD TRAP EXPERIMENTS IN THIS STUDY

22. Two tests were done in our study to determine the accuracy of the MASCOT model. The first test was done with a cold trap similar to the MSA and Fermi designs, and the trap was loaded to plugging with Na_2O. The second cold trap was similar to the typical cold trap configurations used in most U.S. sodium systems today; it was loaded to plugging with hydrogen. Both cold traps were small and were tested on the Apparatus for Monitoring and Purifying Sodium (AMPS) located at Argonne National Laboratory.

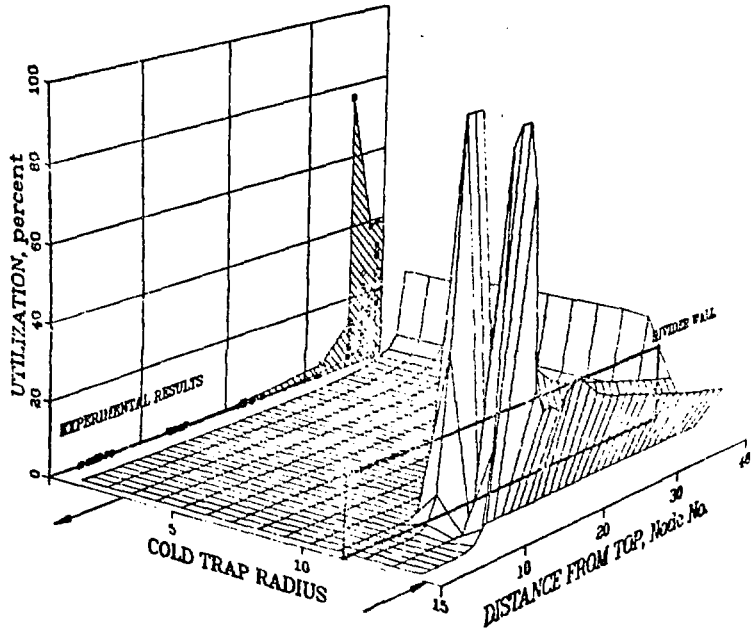

Fig. 7. Impurity mass distribution calculated for the Fermi primary system cold trap compared with the experimental results.

Cold trap ECT1

23. Experimental Cold Trap Number One (ECT1) had a long, thin configuration, as shown in Fig. 8. Sodium entered the top of the annulus and flowed downward through the narrow annulus to the bottom. Flow then reversed, and the sodium entered the bottom of the packed center section and flowed up and out of the trap. The bottom of the trap was attached with a Conoseal flange so that it could be removed after the test for inspection and analysis.

24. Oxygen was added to the AMPS sodium by means of a bed of Na_2O granules that were suspended in a flowing sodium stream in a system side leg. The temperature of the side leg was controlled so that the rate of oxygen dissolution could be controlled to give the desired oxygen concentration in sodium entering the cold trap. Westinghouse-type electrochemical oxygen meters (ref. 7) were located in the sodium stream at the inlet to the cold trap and at the exit. The AMPS was operated at these constant conditions until ECT1 became plugged with Na_2O deposits. The test was then stopped, and ECT1 was removed from the system.

evaporated. Post-test examination indicated that a very thin layer of Na_2O crystals had deposited on the inner surfaces in the annulus and on the bottom cap. A very heavy deposit of Na_2O crystals was observed on the bottom edge of the wire mesh packing.

26. The center section of ECT1 was removed, cut into one-inch segments, and analyzed for both total sodium and elemental sodium. The total sodium less the elemental sodium was used to calculate the amount of Na_2O in each segment. Essentially all of the Na_2O was located in the bottom segment.

27. The operating conditions and geometric configuration of ECT1 were input to MASCOT, and the case was run. The results of the simulation were plotted in the same manner as were previous cases. The Na_2O distribution in ECT1 is shown in Fig. 9, where both the distribution calculated by MASCOT and the experimental results are shown. Note that very little Na_2O is deposited in the annulus in this case, in contrast to the large amounts observed in the MSA and Fermi cases. This effect is probably due to the very low oxygen concentration in the inlet sodium in the ECT1 case as opposed to the

25. The plugged ECT1 was then inverted and connected to the top of a drain tank which was connected to a vacuum system. It was heated to ~630 K (360°C) under vacuum and was maintained at that temperature for 100 h to assure that all the sodium had been

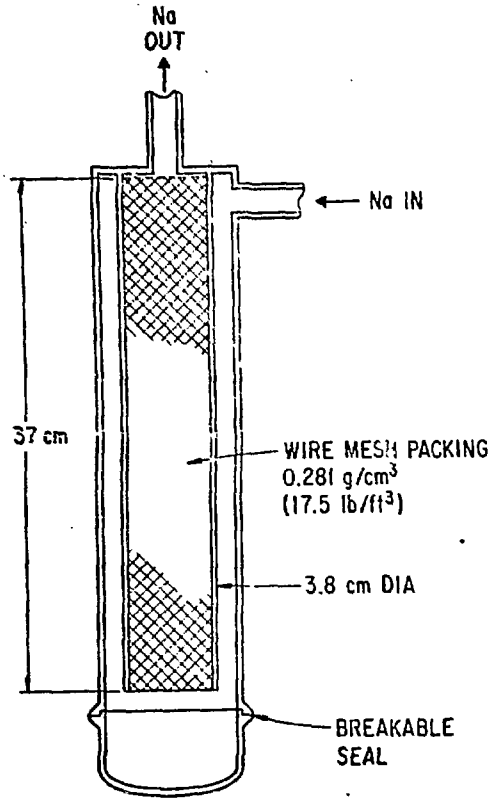

Fig. 8. Design configuration of ETC1.

relatively large concentrations in the MSA and Fermi cases. The low concentration provided a much smaller source of impurities for deposition on the ECT1 walls. Although the annulus walls were not analyzed for quantity of Na_2O, the visual observation confirmed that little deposition occurred in that location. Agreement between the MASCOT calculation and the experimental measurements is excellent.

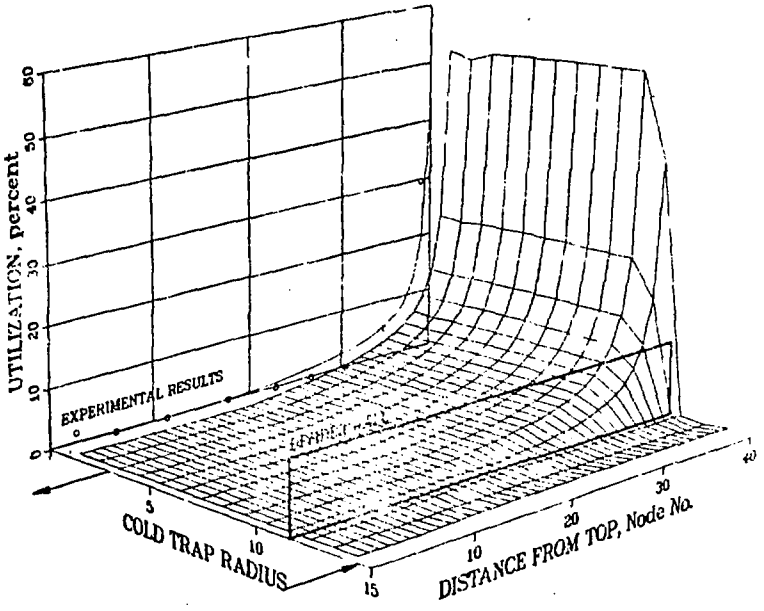

Fig. 9. Impurity mass distribituion in the ECT1 case.

CRBR model cold trap

28. The second cold trap tested in this program was originally designed as a scale model of the cold trap for Clinch River Breeder Reactor (CRBR) Intermediate Heat Transport System (IHTS). The CRBR model cold trap is shown schematically in Fig. 10.

29. The cold trap was loaded under very carefully controlled conditions. Hydrogen was injected into the sodium by diffusion through nickel membranes. Pure hydrogen was introduced into a closed, thin-walled nickel tube at a pressure of ~170 kPa (10 psig), and it diffused through the tube wall into the sodium. Hydrogen concentrations in the sodium entering and exiting the cold trap were measured with diffusion-type hydrogen meters (ref. 1). After the cold trap was loaded with hydrogen samples the mesh sections were taken for analyses. These samples were taken by driving sharpened tubes into the mesh and withdrawing the tubes. The samples were analyzed for hydrogen content.

30. The CRBR model case was run with MASCOT to calculate the expected hydrogen distribution. The results of this calculation are presented in Fig. 11. The hydrogen deposition in this case was essentially all concentrated in the upper part of the annulus region, and the agreement between the model calculation

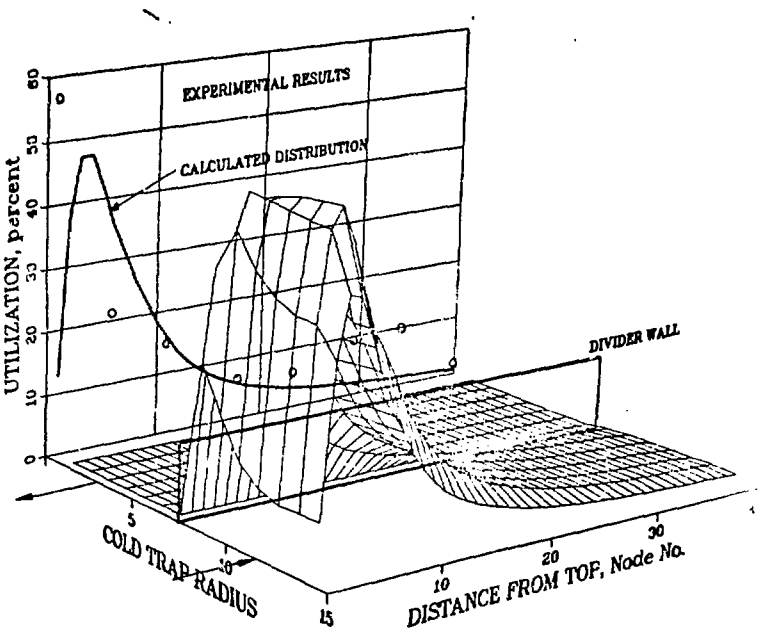

Fig. 11. Impurity mass distribution calculated and measured in CRBR model cold trap case.

DISCUSSION AND CONCLUSIONS

31. The MASCOT has been shown to accurately

presented in Fig. 11. The hydrogen deposition in this case was essentially all concentrated in the upper part of the annulus region, and the agreement between the model calculation and the experimental results is good. The position of the NaH deposit is a direct result of the operating conditions, i.e., the hydrogen concentration at the inlet was high (1.2 ppm) and constant during the entire experiment. This condition resulted in precipitation near the inlet end of the annulus.

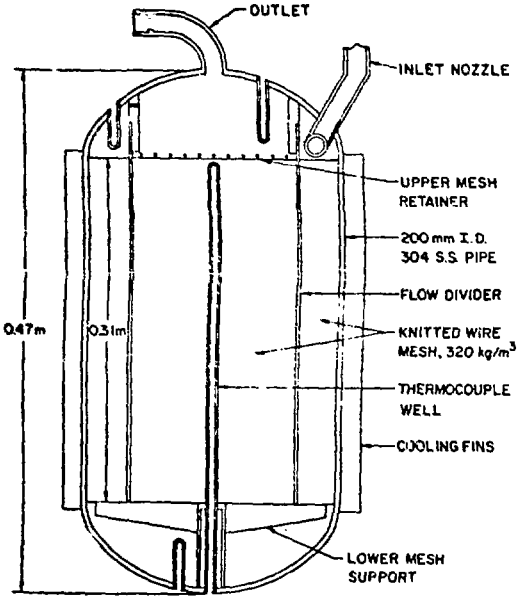

Fig. 10. Configuration of the CRBR model cold trap.

DISCUSSION AND CONCLUSIONS

31. The MASCOT has been shown to accurately calculate the distribution of impurity mass deposits in cold traps, both from data in the literature and from data generated in experiments in this work. Although the general pattern of mass distribution has been shown to be calculated accurately by MASCOT, the absolute values of the concentrations in different positions are not precisely calculated. This failure to calculate accurate concentrations is partially due to lack of accurate historical data; and partially due to the inability of MASCOT to simulate unusual conditions.

32. The conclusions of this study are summarized below:

1. The patterns of impurity depositions in cold traps of a wide variety of designs and operating conditions were simulated very well by MASCOT.
2. The MASCOT simulation was equally good for both hydrogen and oxygen in sodium.
3. Although agreement between calculated and measured mass distributions was good, the absolute values of mass deposition were sometimes different between the two cases.
4. The MASCOT model cannot simulate unusual cold-trap configurations, nor can it handle changes in configuration (such as movement of the mesh) during a run.

5. The MASCOT model will be useful for studying various cold trap configurations and the effect of design variables on the capacity of the cold traps for retaining impurity deposits.

6. The MASCOT model will be useful for assisting cold trap designers to achieve designs that are optimized for specific applications.

33. Some insights into cold trap behavior that have resulted from this study are summarized in the following paragraphs:

1. Narrow flow passages should be avoided in regions where the sodium temperature is being reduced in the impurity-saturation range. Impurities will deposit in these regions and possibly plug the flow passage.

2. A large volume having an abundance of nucleation sites should be provided in the region of the cold trap where precipitation of impurities first begins. This region will accumulate most of the impurity burden of the sodium system.

3. Cold trap designs having no packing where the sodium is cooled below the impurity saturation temperature and having packing downstream of the cooling region will generally have low capacity. This low capacity is due to the sodium becoming supersaturated in the packless region followed by rapid precipi-

REFERENCES

1. VISSERS D. R., HOLMES J. T., BARTHOLME L. G. and NELSON, P. A. A hydrogen-activity meter for liquid sodium and its application to hydrogen solubility measurements, Nucl. Technol. 1974, 21, March, 235.
2. MCKEE J. M. Water-to-sodium leak detector: development and testing, Proceedings of International Conference on Liquid Metals Technology in Energy Production, Champion, Pa, CONF-760503-P2, 1976, May.
3. ROGERS D. N., et al., Sodium concentration and departure from nucleate boiling in the clinch river breeder reactor plant, AIChE 17th National Heat Transfer Conference, Salt Lake City, UT, 1977, August.
4. BILLURIS G Experimental investigations of the removal of sodium oxide from liquid sodium, General Electric Company, San Jose, CA Report GEAP-3328, 1960, January.
5. ROGERS S. J., PALLADINO C. A. and WILDEMAN T. J. Analysis of high oxygen and high carbon cold traps - topical report no. 9, MSA Research Corporation, Evans City, PA Report MSAR 67-203, 1967, December.
6. HERB J., et al., Examination of the enrico fermi sodium cold trap, Westinghouse Electric Corporation, Pittsburgh-

where the sodium is cooled below the impurity saturation temperature and having packing downstream of the cooling region will generally have low capacity. This low capacity is due to the sodium becoming supersaturated in the packless region followed by rapid precipitation of impurities when the packing is encountered. The packing provides many sites for nucleation and growth of inpurity crystals.

4. The center section collects very little impurity deposits in a cold trap that has packing in the annulus, and a cold trap having no packing in the annulus plugs quickly in the center section. Therefore, a preferred design would have a large, packed annulus region and a relatively small, unpacked center region.

ACKNOWLEDGMENTS

34. The authors wish to express thanks to Dr. F. A. Cafasso, Manager of the Sodium Technology Program, to R. Land and S. Gabelnick for assistance in the computer effort, to R. Kumar for helping to develop the three-dimensional plotting routines to R. Wolson and V. Kolba, who are continuing this work, and to M. Homa, F. Williams, and K. Jensen of the Analytical Chemistry Laboratory.

and high carbon cold traps - topical report no. 9, MSA Research Corporation, Evans City, PA Report MSAR 67-203, 1967, December.

6. HERB J., et al., Examination of the enrico fermi sodium cold trap, Westinghouse Electric Corporation, Pittsburgh, PA Report WCAP-4321, 1965, November.
7. MCKEE J. M., VISSERS D. R. and NELSON P. A. of Argonne National Laboratory and GRUNDY B. R., BERKEY E. and TAYLOR G. R. of Westinghouse Electric Corporation, Calibration stability of oxygen meters for LMFBR sodium systems, Nuclear Technology 1974, 21, March, 217.